

Research Article

Solvent Penetration Rate in Tablet Measurement Using Video Image Processing

D. Braido,¹ Y. Gulak,^{1,2} and A. Cuitino¹

Received 28 October 2011; accepted 28 February 2012; published online 17 March 2012

Abstract. We describe a simple technique for the measurement of solvent penetration rates into spray-dried lactose (DCL) tablets and tablets made of blended materials using digital video image processing. The results of the experimental study show that the penetration rate in some cases appears to be close to linear with time, which corresponds to non-Fickian or Case II-type diffusion. We discuss relevant capillary invasion models in order to explain the observed penetration rate. The proposed technique allows fast diffusion rate acquisition/processing and can be useful when designing immediate release tablets that require a large number of measurements corresponding to different formulations and processing parameters.

KEY WORDS: diffusion; image processing; penetration rate.

INTRODUCTION

The performance of drug delivery systems, such as pharmaceutical tablets, is usually quantified by the dissolution rates required to maintain the desired active ingredients concentration in the gastrointestinal tract. The dissolution rate may be influenced by disintegration of the tablet, but this is not always the case, especially for controlled release systems. Whether or not the tablet matrix disintegrates, the rate at which solvent penetrates the matrix can be highly influential in terms of the drug release rate as well as the total drug released. The solvent/water penetration rate into the tablet often correlates well with the disintegration rate (1). A swelling gel layer, formed during the penetration and acting as a diffusion barrier for active ingredients, may also affect their dissolution rate. Therefore, experimental measurements of the velocity of the liquid front are needed in order to adjust or optimize the drug performance. In addition, such measurements can help us understand the diffusion mechanism for a particular solvent–tablet matrix combination. It is observed that the mass transport through the polymer matrix often deviates from the Fickian diffusion theory, which predicts that the solvent front should advance as a square root of time. In contrast, a Case II mechanism, characterized by a sharp front moving linearly with time and practically uniform solvent concentration behind the front, is observed (2,3). The transitional non-Fickian behavior, called anomalous diffusion, is also possible, but can be hard to observe (4).

A number of experimental techniques have been developed for diffusion studies in polymers (5), consisting of two basic types of investigation: the diffusion front rates and the concentration profile measurements. Clearly, time-dependent

solvent concentration profiles can provide more complete information about the diffusion mechanism but are difficult to obtain and require quite sophisticated and expensive techniques such as nuclear magnetic resonance imaging, light and electron microscopy, Raman spectroscopy, and other methods described in (5). Since the penetrating front is usually sharp, a wider choice of interface tracking methods is available that allows one to avoid the detailed concentration field measurements. One such technique, the ultrasound method (6), offers the possibility of continuous measurement of both the swelling and eroding fronts. A majority of the existing methods, however, require expensive equipment, special tablet samples preparation, and time consuming data collection and processing. In the present work, we describe a simple technique of practical nature for solvent diffusion front tracking by visualizing the penetration process using digital video image processing. The goal is not a comprehensive study of a particular sample, but rather a fast diffusion rate estimation and comparison in multiple tablets of different formulations or process parameters. This technique is especially suitable for immediate release tablets that show relatively fast solvent penetration rate. It works well with commonly prepared tablets (i.e., compressed using a rotary tablet press) and does not necessarily require special samples preparation. Most of our results show close to linear penetration front advance that correspond to the non-Fickian or Case II sorption.

It should be noted, that in some studies, the sorption ability of tablets is determined by measuring the absorbed mass M with time t using standard tensiometers (7). Then, a velocity constant K is obtained by fitting the experimental data to the Washburn-like equation (8).

$$M^2 = Kt \quad (1)$$

Morrissey and Vesely (9) argue, however, that the measurements of mass uptake are less valuable, since they cannot

¹ Mechanical and Aerospace Engineering, Rutgers University, Piscataway, New Jersey 08854, USA.

² To whom correspondence should be addressed. (e-mail: ygulak@jove.rutgers.edu)

differentiate between the concentration level and the penetration distance. In addition, the question of applicability of the Washburn model to the case of non-Fickian sorption requires special attention and will be discussed below.

There are several theories/models of the non-Fickian diffusion that can be used to interpret/fit the experimental penetration data (for recent overviews see (5,10)). One such theory, developed by Thomas and Windle (11), recognizes that the kinematics of the penetration is controlled by the rate at which the polymer structure rearranges or relaxes due to the solvent moving in. Wu and Peppas (12) extended the Thomas and Windle model by introducing a coupling between mass transport, driven by the concentration gradient and deformation in the polymer, based on the continuum mechanics formulation. They employed the Maxwell viscoelastic stress-strain constitutive relations so that a polymer relaxation time could be naturally defined. This model can describe a transition from Fickian to Case II transport depending on which process—solvent diffusion in a swollen polymer region or stress relaxation in the glassy region—advances at a slower rate. It is mathematically formulated as a boundary value problem for a system of coupled partial differential equations (PDEs) from which the time evolution of the concentration and stress fields can be obtained numerically (13). However, while the Wu–Peppas and similar models capture well physical mechanisms of the penetration and are supported by experimental evidence, they are not widely used in practice. One reason for that is the technical complexity of fitting PDEs to the experimental penetration data. Also, such models contain several empirical relations with parameters that are difficult to measure, for example, concentration-dependent diffusion and viscosity coefficients.

We also examine an alternative approach for describing the penetration process and experimental data treatment. The key idea is that the diffusion rate is mainly controlled by the resistance of the polymer matrix to the solvent flow, which is put forward in the molecular sorption model proposed by Vesely (14,15). This model visualizes the polymer matrix as a porous media containing voids filled by the solvent with the molecular interactions between the polymer and solvent molecules resulting in an internal pressure, similar to the capillary pressure. Thus, the penetrant motion is driven by the capillary pressure with the contact angle θ , opposed by the viscous resistance forces.

Using the results from an inexpensive method for determining solvent penetration into compacts of organic particulate systems, we compare these results to the two numerical models of Washburn and Vesely.

MATERIALS AND METHODS

The first set of tablets is composed of directly compressible lactose (DCL), specifically SuperTab 14SD obtained from DMV Fonterra. The tablets are prepared using a custom manual hydraulic press comprised of an Enerpac P392 hydraulic hand pump and cylinder which actuates a steel stage from the bottom and a Delta Metrics XLP58-020K force transducer located above the moving stage. An LCD display shows the current force being registered by the transducer at all times during the compaction process. In order to ensure the outer surfaces were free of imperfections and that no lubricant would be necessary in the DCL powder, tablets are compressed at much slower speeds than could be readily achieved

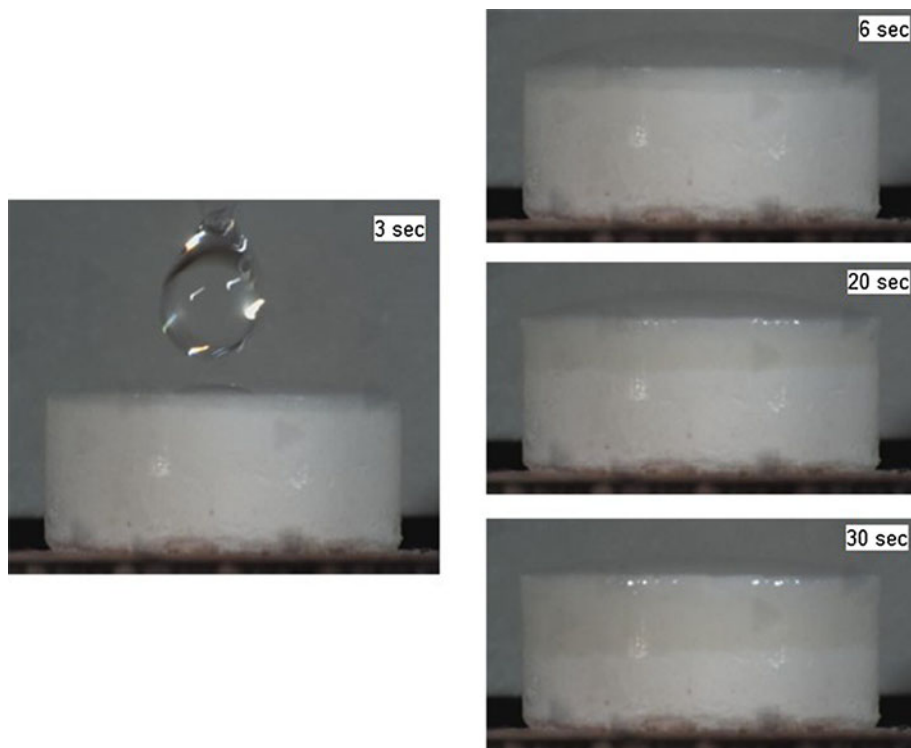


Fig. 1. Sequence of collected images showing the solvent penetration at different moments of time

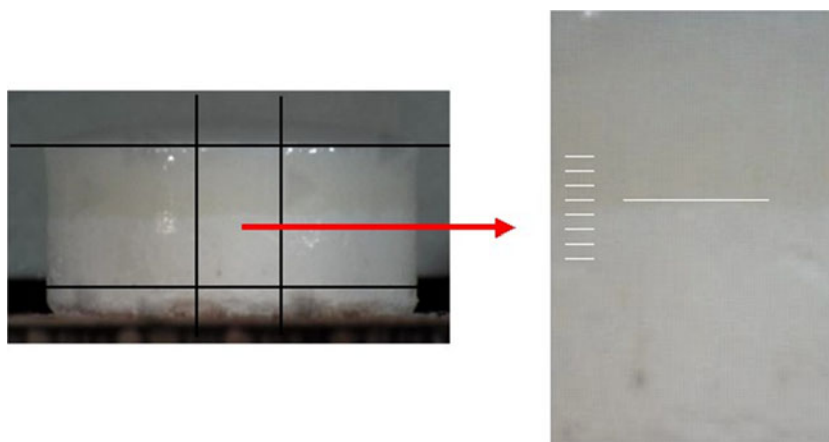


Fig. 2. Rectangular region of 300×200 pixels selected for image analysis

using a rotary tablet press or simulator. Attempts to use either of these alternate platforms resulted in tablets shattering upon ejection.

A 10-mm flat faced punch and die set made of polished S7 steel is used. Each tablet is made by weighing out 400 ± 4 mg of DCL on an Ohaus digital balance. The filled die is placed in the hydraulic press and the pump operated until the target force is reached. The actual compression takes place over a period of approximately 10 s, and the applied force is held constant for 10 s before the pressure is released. As the press is manually pumped, the exact time of the compression event cannot be controlled; however, it occurs at a speed which is sufficiently slower than the assumed relaxation time of the powder such that the compaction process can be assumed equivalent for each set of tablets. Once the powder is compacted, the die is placed on top of a hollow cylinder inside the press and pressure reapplied until the tablet is released from the die. The force required to remove the tablet was never greater than 1 kN. After removal of the tablet, the die set is cleaned with water, then methanol and wiped before reuse. The resulting tablets are examined to ensure the surfaces are defect free, then weighed and measured for thickness and diameter. Any tablet which falls outside of the prescribed tolerances of mass (400 ± 4 mg) or thickness (4.00 ± 0.05 mm) is discarded immediately. Six tablets are selected from those produced in the hydraulic press for hardness testing. These tablets are allowed to rest for about 1 h after compaction before measuring mass (balance portion of Pharmatron Auto Test 4), thickness and diameter (Mitutoyo Digital Calipers, CD-6" CX) and hardness (Pharmatron Tablet Tester 6100D).

The other tablets investigated are made of blended material containing Avicel, lactose, fumed silica (glidant), magnesium stearate (lubricant), and chlorpheniramine maleate (active ingredient), prepared in the manner described in Pingali *et al.* (17), herein referred to as Chlorphen. For our purposes, the two extreme processing conditions were selected, 40 rpm–40 rev and 160 rpm–640 rev as these are expected to be the most different in terms of performance as evidenced by their respective dissolution. The blends are compressed using a Presster tablet press simulator set to model a Kikisui Libra2 press moving at 60 rpm. A 10-mm, round, flat-face, B-type, D2 steel tooling (Natoli Engineering Co., Inc.) is used. The tablet mass is 405 ± 3 mg and compaction force is either 8 ± 4 kN or 13.8 ± 4 kN.

Precompaction force is minimal and kept below 1 kN. A set of compaction curves are produced by making tablets of each blend at multiple compaction pressures and then measuring mass, thickness and diameter, and hardness (same equipment as previously described).

To monitor the penetration distance, we perform simple experiments by carefully depositing $50 \mu\text{L}$ (for DCL14SD tablets), $75 \mu\text{L}$ (for Chlorphen tablets) of distilled water in the center of the top surface of the tablet using a metered micropipette (Eppendorf Reference model E2000-100 with disposable tips). The amount of water is chosen so that it does not flow over the side of the tablet, but still creating conditions where a high concentration remains on the top surface until the solvent interface penetrates about half of the tablet

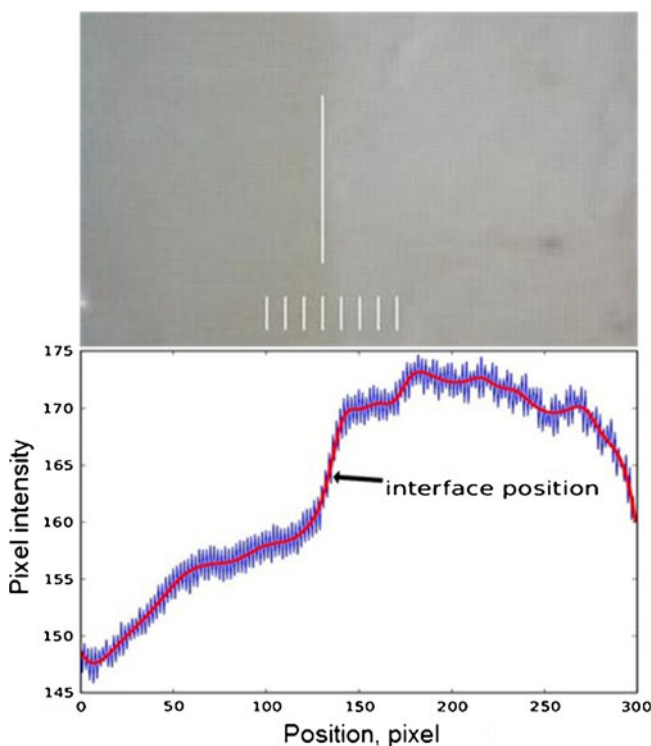


Fig. 3. Average pixel intensity curve over the selected region width obtained using smoothing splines

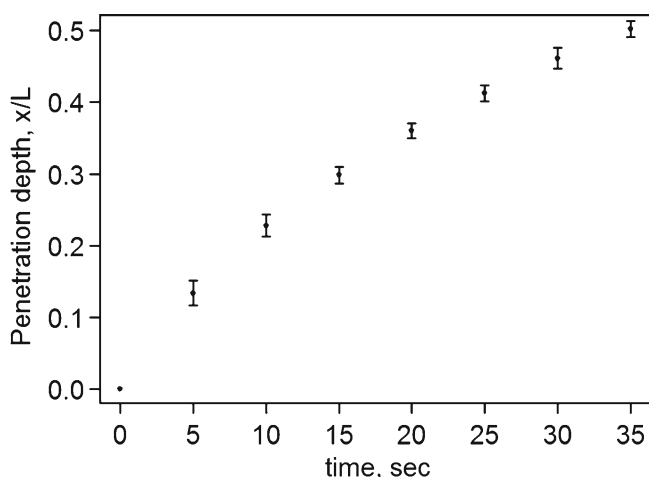


Fig. 4. Penetration depth with time measured for tablets compressed with the compression force of 4 kN

thickness, approximately 2–3 mm. This is done to ensure solvent penetration progresses exclusively through the top face of the tablet, effectively reducing the experiment to a one-dimensional characterization. For the hand pressed DCL14SD tablets, this experiment is performed approximately 1 h after the tablets are compressed, whereas for the Chlorphen tablets this experiment is performed within 2–3 min after compaction.

All tablets are measured for mass, thickness, and diameter (same equipment as previously described) immediately before performing penetration tests. Sample size for each group is eight tablets, except for the high compression force Chlorphen tablets which have a sample size of 4. To film the penetration, we used a GimaGo GO443C camera positioned to capture the cylindrical side wall of the tablet. Figure 1 shows a typical sequence of collected images. The GimaGo camera is connected via a Cat-5 cable to the network card of a desktop computer running Windows 7. Videos are captured and stored using the Xvid codec. We used the OpenCV (16) computer vision library in Python to extract the interface position with time from the collected images comprising the videos as follows. First, the color images are converted to grayscale, and a rectangular area with a width of about 200 pixels along the tablet thickness is selected for analysis, as shown in Fig. 2. Then, the average pixel intensity over the width of the chosen area is calculated and the noise is eliminated from the resulting curve using smoothing splines. Finally, edge detection of the first and second derivatives defines

the position of the interface (Fig. 3). The described algorithm was programmed and can run, in principle, in batch mode to process many images at once. We noticed, however, that different images require varying degree of smoothness for the noise elimination due to glare from lighting. Thus, in order to ensure a more accurate capturing of the interface position, we performed the smoothing step interactively and checked the results with visual inspection of the images periodically.

RESULTS

The DCL tablets have an average tensile strength of 0.91 MPa tensile strength with a standard deviation of .0089 MPa at the compaction force of 4 kN (51 MPa compaction pressure). This is just under 1% of variability. These data combined with the acceptance of only tablets which fell within specified criteria allow us to assume the remaining DCL tablets are sufficiently similar in terms of physical properties.

Figure 4 shows the measured penetration distance data for tablets compressed with the compression force of 4 kN. The curve is initially fairly linear but decays over time. This decay may be the result of several factors, such as the decrease in concentration of fluid as it is spread over a larger volume or dissolution of lactose into the water changing its chemical composition. We do not explore the exact nature of this decay in this work. Of particular note is the consistency of the penetration results. The standard deviations are small as compared to the magnitudes of the measurements. As the tablets examined are composed of a single component and are prepared in an identical and repeatable manner, the variability of the technique is minimal, and differences in measurements between future, less identical, samples is most likely due to differences in the samples as opposed to noise in the measurements.

The Chlorphen tablets are slightly more variable in terms of properties. Figure 5 shows the compaction profile of both processed Chlorphen blends being investigated. At the lower compaction force (8 kN, ~100 MPa pressure), the ratio of compaction pressure to tensile strength is very similar for both blends; however, at the higher force (14 kN, ~170 MPa pressure) the difference in ratios is noticeable with the 640 rev batch achieving less tensile strength at even greater compaction pressures.

Similar agreement can be seen in the penetration results of the low compaction force sample tablets made from Chlorphen blends, though tablet variability appears to be more prevalent than for the monocomponent tablets. Figure 6 shows the penetration results from the Chlorphen tablets from both blends at

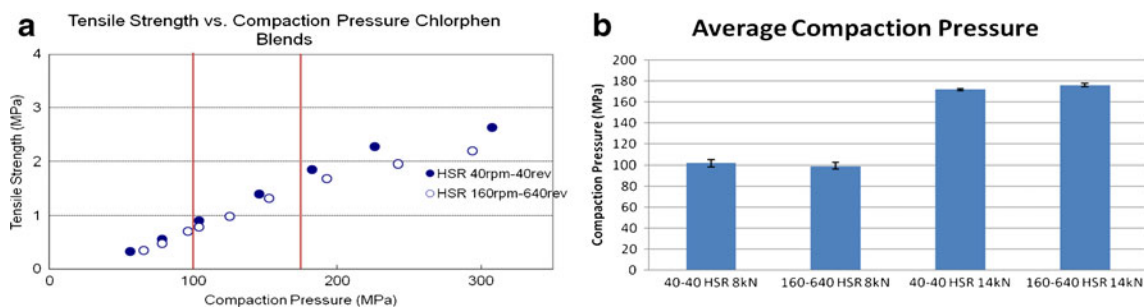


Fig. 5. a Compaction performance of processed Chlorphen blends. **b** Compaction performance of Chlorphen tablets used in penetration experiments

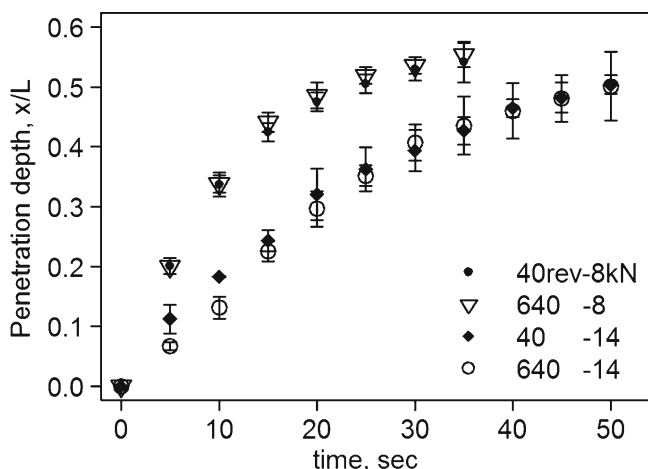


Fig. 6. Solvent penetration results for Chlorphen blend tablets

both compaction pressures. The results show the effect of compaction pressure on solvent penetration rate. There appears to be no real differences in the initial solvent penetration rate between the two different blends at low compaction pressures. The divergence at later time points is small and appears to be an effect of the plateau position of the solvent penetration. While the 8 kN compaction force Chlorphen tablets are of nearly identical size and density, they most likely have different microstructures which influence this plateau (17). At the higher compaction force, the Chlorphen tablets of the two blends exhibit initially different and close-to-linear solvent penetration rates but later have similar plateau regimes. The 640 rev blend has been shown to be more hydrophobic than the 40 rev blend in the works of Llusa *et al.* (18). This only appears to affect the initial rate of solvent penetration in the more compacted (14 kN) tablets, while the less compacted (8 kN) tablets show no appreciable effect. These results are similar to the dissolution performance of similarly processed blends of nearly identical materials (17). Furthermore, at the higher compaction forces, tablets made from the 640 rev blend have lower tensile strength than tablets made from the 40 rev blend, but allow solvent to progress through marginally slower than for tablets made from the 40 rev blend. It would be assumed that the lower tensile strength tablets would be more apt to allow solvent to penetrate their matrix.

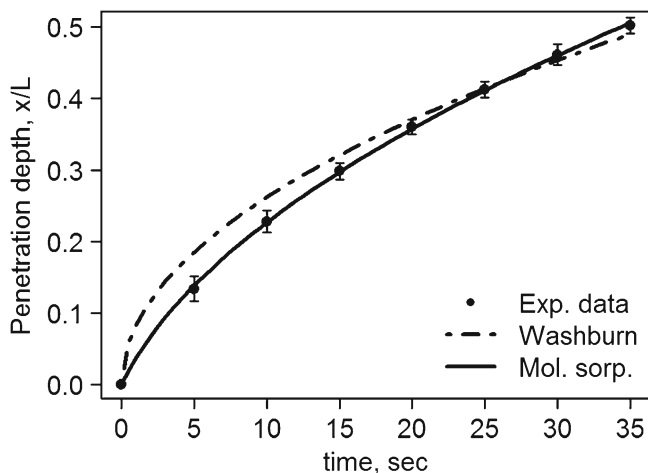


Fig. 7. Model fits for tablets of pure DCL (Washburn: $k=0.00686$; Mol Sorp: $k=0.634$, $B=0.133$)

DISCUSSION

As previously stated, we use the Washburn and molecular sorption models to interpret the results of our experiments. Both models are based on the capillary tube invasion idealization. The Washburn model considers penetrant motion to be determined by the balance between capillary pressure with the contact angle θ and the viscous Hagen–Poiseuille pressure loss:

$$\frac{2\sigma \cos \theta}{R} = \frac{8\mu x}{R^2} \dot{x}. \quad (2)$$

Here x refers to the variable diffusion distance, R to the capillary radius, μ to the dynamic viscosity, σ to the surface tension. Integrating Eq. 2 with the initial condition $x(0)=0$ leads to the well-known Washburn equation (8):

$$x^2 = \frac{\sigma R \cos \theta}{2\mu} t. \quad (3)$$

This equation, however, fails for short times since the initial velocity $\dot{x} \propto 1/\sqrt{t}$ diverges at $t \rightarrow 0$. To fix the initial diffusion rate, Vesely (14,15) makes an assumption that the diffusion

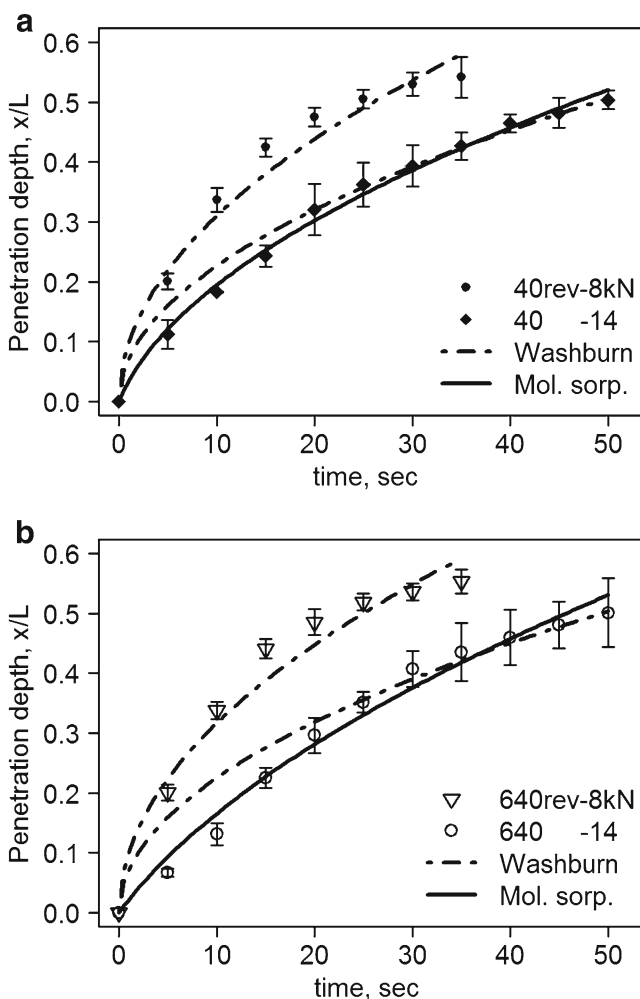


Fig. 8. **a** Model fits for tablets of low total strain blends. (Washburn (8,14): $k=0.00962$, 0.00514 ; Mol Sorp (14): $k=0.896$, $B=0.0903$). **b** Model fits for tablets of high total strain blends (Washburn (8, 14): $k=0.0100$, 0.00507 ; Mol Sorp (14): $k=0.182$, $B=0.244$)

starts at some nonzero distance B thus the modified momentum Eq. (2) becomes $\dot{x} = A/(x + B)$, where constant $A = \sigma R \cos \theta / 4 \mu$. The solution of this equation with the initial condition $x(0) = 0$ gives the final expression of the molecular sorption theory:

$$x = B \left(\sqrt{kt + 1} - 1 \right), \quad (4)$$

here $k = 2A/B^2$ is the scaling constant. Equation 4 accurately fits the penetration distance measurements corresponding to the Fickian, as well as Case II diffusion (14,15). This can be explained by a Taylor series expansion of the square root term that gives:

$$x \cong Bkt/2, \quad (5)$$

valid at the initial time when $kt \ll 1$. Thus, for sufficiently small values of k , the penetration curve might look like a linear function on some finite time interval.

Figure 7 shows the best fits of these two models to the solvent penetration results from the DCL tablet experiments. The molecular sorption model appears to provide a rather high fidelity fitting of the results, well within the experimental error. By contrast, the Washburn model does not fit within experimental error. The initial slope of the Washburn model causes the fit to deviate from the experimental results, and it is unable to overcome this deviation until much later.

Fitting data from the processed blends proved to be slightly less effective. For the lower compaction force tablets from both blends, it was not possible to fit the molecular sorption model to the experimental results.

Figure 8a shows the fit of the models to the solvent penetration results of tablets made from the low strain blend. At the higher compaction force, the molecular sorption model provides an acceptable fit of the data. The Washburn model fit the experimental results poorly for either compaction condition. In the case of the high compaction force tablets, the Washburn equation was only a poor initial fit, and rectifies itself to a better fit once the solvent penetration rate begins to decay.

Figure 8b shows the fit of the models to the solvent penetration results of tablets made from the high strain blend. Neither model provides a good fit to the experimental results over the complete time interval at either compaction force. Initially, for the high compaction force tablets, the molecular sorption model more closely resembles the data, while the Washburn model is a better fit at later time points. This blend is a complex, multicomponent, highly processed system, and the lack of fit to either model points to the existence of mechanisms which are not incorporated.

CONCLUSION

We have presented an experimental technique for the measurement of the solvent/water penetration in immediate release tablets using digital video image processing. This technique may be useful if many tablets have to be processed and their absorption ability compared. The solvent penetration front is tracked explicitly using this technique. The solvent penetration results of a simple system fit well with the molecular sorption model proposed by Vesely; however, the lack of direct correlation of the coefficients with actual physical parameters limits the insights which can be gleaned from this

model. The more complex systems produce more variable results. For higher compaction forces, the molecular sorption model provides a better fit with the data while at lower compaction forces the Washburn model more closely resembled the data. For tablets made from more complex powder blends, the mechanisms governing penetration are not completely incorporated in either model utilized herein.

ACKNOWLEDGMENTS

The authors are grateful to the National Science Foundation (EEC 0540855, CDI 0941302-CBET), and U.S. Food and Drug Administration/National Institute for Pharmaceutical Technology and Education (HHSF223200810029C) for providing funds for this research.

REFERENCES

1. Massimo G, Catellani PL, Santi P, Bettini R, Vaona G, Bonfanti A, *et al.* Disintegration propensity of tablets evaluated by means of disintegrating force kinetics. *Pharm Dev Technol.* 2000;5(2):163–9.
2. Alfrey Jr T, Gurnee EF, Lloyd WG. Diffusion in glassy polymers. *J Polym Sci C.* 1966;12:249–61.
3. Crank J. The mathematics of diffusion. 2nd ed. Oxford: Clarendon Press; 1975.
4. McDonald PJ, Godward J, Sackin R, Sera RP. Surface flux limited diffusion of solvent into polymer. *Macromolecules.* 2001;34:1048–57.
5. Vesely D. Diffusion of liquids in polymers. *Int Mater Rev.* 2008;53(5):299–315.
6. Konrad R, Christ A, Zessin G, Cobet U. The use of ultrasound and penetrometer to characterize the advancement of the swelling and eroding fronts in HPMC matrices. *Int J Pharm.* 1998;163:123–31.
7. Luginbühl R, Leuenberger H. Use of percolation theory to interpret water uptake, disintegration time and intrinsic dissolution rate of tablets consisting of binary mixtures. *Pharm Acta Helv.* 1994;69(3):127–34.
8. Washburn EW. The dynamics of capillary flow. *Phys Rev.* 1921;17(3):273–83.
9. Morrissey P, Vesely D. Accurate measurement of diffusion rates of small molecules through polymers. *Polymer.* 2000;41:1865–72.
10. Bond DA, Smith PA. Modeling the transport of low-molecular-weight penetrants within polymer matrix composites. *Appl Mech Rev.* 2006;59:249–68.
11. Thomas NL, Windle AH. A deformation model for Case II diffusion. *Polymer.* 1980;21:613–9.
12. Wu JC, Peppas NA. Modeling diffusion in glassy polymers with an integral sorption Deborah number. *J Polym Sci B.* 1993;31:1503–18.
13. Wu JC, Peppas NA. Numerical simulation of anomalous penetrant diffusion in polymers. *J Appl Polym Sci.* 1993;49:1845–56.
14. Vesely D. The rate of solvent diffusion in amorphous polymers. *Macromol Symp.* 1999;138:215–23.
15. Vesely D. Molecular sorption mechanism of solvent diffusion in polymers. *Polymer.* 2001;42:4417–22.
16. Bradski G. The OpenCV library. Dr. Dobbs J Soft Tools [Internet]. 2000 Nov [cited 2011 Aug 15]. Available from: <http://drdobbs.com/open-source/184404319>
17. Pingali K, Mendez R, Lewis D, Michniak-Kohn B, Cuitino A, Muzzio F. Evaluation of strain-induced hydrophobicity of pharmaceutical blends and its effect on drug release rate under multiple compression conditions. *Drug Dev Ind Pharm.* 2011;37(4):428–35.
18. Llusa M, Mehrotra A, Faqih A, Levin M, Muzzio FJ. Influence of shear intensity and total shear on properties of blends and tablets of lactose and cellulose lubricated with magnesium stearate. *Int J Pharm.* 2007;336:284–91.